

25 **Abstract**

26

27 Spatiotemporal trends in pro-inflammatory (interleukin (IL)-6 and IL-8) release after exposure to the
28 water-soluble fractions (WSFs) of PM_{2.5} sampled in 10 large Chinese cities over 1 year were investigated.
29 Chemical components (water-soluble ions, metal(loid) elements, water-soluble organic carbon (WSOC),
30 humic-like substances (HULIS), and endotoxins) in PM_{2.5} samples were measured, and the molecular
31 structure of WSOC was also analyzed by nuclear magnetic resonance. Changes in DNA methylation and
32 gene expression of candidate genes were also evaluated to explore the potential mechanisms. PM_{2.5} from
33 southern cities induced lower pro-inflammatory responses than those from northern cities. Seasonal
34 differences in toxicity were noted among the cities. IL-6 was significantly correlated with HULIS (as the
35 main fraction of WSOC with oxygenated carbohydrate structures characteristic), Pb and endotoxin.
36 Furthermore, DNA methylation and gene expression changes in *RASSF2*, and *CYP1B1* were related to
37 pro-inflammatory secretion. Certain components of PM_{2.5}, rather than PM_{2.5} mass itself, determine the
38 pro-inflammatory release. In particular, HULIS, which originated from primary biomass burning and
39 residual coal combustion, and secondary organic aerosols, appear to be the key component in PM_{2.5} to
40 induce human health risk.

41

42 Keywords: HULIS; NMR; PM_{2.5}; Spatiotemporal; DNA methylation

43

44 **1. Introduction**

45 Fine particulate matter (PM_{2.5}) causes respiratory and cardiovascular disease¹. Inflammatory activity
46 is considered to be the first biological reaction to PM_{2.5} exposure, which could induce these diseases². As
47 such, *in vitro* human cell culture models have been used widely to evaluate the ability of PM_{2.5} to trigger
48 pro-inflammatory activity³. It has been reported that the water-soluble fraction (WSF) which accounts for
49 the major proportion of PM_{2.5}⁴, induces more abnormal biological outcomes than water-insoluble PM_{2.5}
50 components^{5,6}.

51 Identifying the potential fractions and components of PM_{2.5} with the ability to induce
52 pro-inflammatory activity change is critical in atmospheric research, and several studies have assessed the
53 relationships between chemicals in PM and toxicity *in vitro*. For example, metal (loid)s (e.g., Cr, Al, Si, Ti,
54 Fe, and Cu), ions (K⁺ and NH₄⁺), and polycyclic aromatic hydrocarbons (PAHs) showed significant
55 relationships with toxicological outcomes in studies done in Finland⁷, Mexico³, and Italy⁸. However, the
56 WSF of PM_{2.5}, aside from water-soluble ions and metal (loid)s which can be measured individually,
57 contains numerous organic compounds (which are not easy to be fully identified in the WSF), which
58 probably make a significant contribution to pro-inflammatory activity⁹. For instance, humic-like
59 substances (HULIS), consisting of high-molecular-weight organic compounds and represent the main
60 fraction of water-soluble organic carbon (WSOC) in PM_{2.5}, can induce reactive oxygen species (ROS), as
61 shown by the dithiothreitol (DTT) assay^{9,10}. Therefore, identification of the major types of organic matter
62 and the molecular groups therein, represents an alternative approach to comprehensively determine
63 pro-inflammatory organic components. Nuclear magnetic resonance (NMR) spectroscopy is considered as

64 a method to explore the molecular structural characteristics of organic components within a matrix¹¹.

65 In China, about 83% of people are currently living in the areas with PM_{2.5} concentrations exceeding
66 the Chinese Ambient Air Quality Standard (35 µg/m³), and 1.37 million premature adult mortalities in
67 2013 may be attributable to air pollution¹². However, there are limited data on the relationship between
68 PM_{2.5} components and pro-inflammatory activity in China¹³.

69 The mechanisms linking PM_{2.5} exposure to pro-inflammatory release have been not fully understood¹⁴.
70 DNA methylation could be altered by environmental factors and can median this impact on a phenotype
71 and disease¹⁵. Indeed, DNA methylation is thought to be related to air pollution toxicity due to the
72 significant relationships between the changes in DNA methylation of several genes with PM exposure in
73 several epidemiological studies^{14,16}. Moreover, the modifiable characteristics of DNA methylation most
74 likely render protective measures, and could be applicable for new drug development¹⁷.

75 In this study, PM_{2.5} samples from 10 large cities in China were collected during 1 year (2013–2014)
76 and the WSFs of pooled PM_{2.5} samples were used to evaluate their ability to induce pro-inflammatory
77 activity in the human cell models. In addition, we characterized the inorganic and organic components of
78 the WSF of PM_{2.5}. Organic components (i.e., WSOC and HULIS) were quantified and the structural
79 characteristics of WSOC were qualified using NMR. Furthermore, the relationships between the
80 components of PM_{2.5} and their molecular structural characteristics were evaluated, and the DNA
81 methylation mechanism were also explored, since this may help identify novel therapeutic targets against
82 PM_{2.5} exposure.

83

84

85 **2. Methods**

86 *2.1 PM_{2.5} sampling, organic fraction extraction, and WSF extraction*

87 PM_{2.5} samples were collected from 10 urban cities in China (Beijing (BJ), Shanghai (SH),
88 Guangzhou (GZ), Nanjing (NJ), Wuhan (WH), Taiyuan (TY), Chengdu (CD), Lanzhou (LZ), Guiyang
89 (GY), and Xinxiang (XX)) during spring (SP), summer (S), autumn (A), and winter (W). Detailed
90 descriptions of the sampling sites, sampling methods, and protocols are given in our previous paper¹⁸.
91 Densely inhabited districts in the cities were selected for sampling. And sampling sites were set up on
92 rooftops approximately 15–20 m above ground level. PM_{2.5} were collected using 20.3 × 25.4 cm prebaked
93 (5 h at 450 °C) Whatman quartz microfiber filters (QFFs). Samples were collected during October 22 2013
94 to November 13 2013 for autumn (total 22 samples), December 30 2013 to January 20 2014 for winter
95 (total 20 samples), March 30 2014 to April 20 2014 for spring (total 22 samples), and June 26 2014 to
96 August 24 2014 for summer (total 28 samples), respectively. Each piece of filter was recorded the
97 sampling time and rate, which was used to calculate the volume of sampling air. During each season, 24-h
98 integrated PM_{2.5} samples were collected. And a circle with 2.75 cm radius was cut from each piece of
99 filters and then was pooled into a single sample for each season. Thus, 38 samples were used in the
100 subsequent experiments (except GY, where only SP and S samples were collected).

101 Two PM_{2.5} samples from Guangzhou City in the winter of 2013 was collected using a PM_{2.5} sampler.
102 Combustion of corn stalks was collected through a sampling system¹⁹. Coal combustion was done with a
103 high-efficiency stove with a PM_{2.5} dilution sampling system¹⁹.

104 The WSF fraction was extracted from PM_{2.5} samples by sonication using deionized water. The extract
105 was filtered through a 0.22 μm filter, freeze dried, and dissolved in deionized water. More details are
106 presented in S1-1.

107 The dichloromethane (DCM) fraction was extracted from PM_{2.5} samples collected in GZ in 2013 (GZ

108 W1 and GZ W2). PM_{2.5} samples were collected from the combustion products of corn stalks, coal, and
109 vehicle exhaust. The filters were then extracted with DCM using pressurized liquid extraction (ASE300;
110 Dionex Corp., Sunnyvale, CA, USA) for 2 days. Finally, the extracts were gently evaporated and dried
111 under nitrogen gas and reconstituted with dimethyl sulfoxide to various concentrations.

112 *2.2 Inorganic chemical analyses*

113 Ion chromatograph (883 Basic IC Plus; Metrohm, Herisau, Switzerland) was used to analyze Six
114 cations (Li⁺, Na⁺, NH₄⁺, K⁺, Mg²⁺, and Ca²⁺) and seven anions (F⁻, Cl⁻, Br⁻, NO₂⁻, PO₄⁻, NO₃⁻, and SO₄²⁻),
115 and ICP-AES (VISTA-MPX; Varian, Palo Alto, CA, USA)⁶ was used to measure the 13 metal (loid)
116 elements. Details are shown in the SI. The result of each chemical are expressed as μg/m³, and the blank
117 filter was used as the blank, whose chemicals concentrations were subtracted.

118 *2.3 Organic fraction measurement*

119 The WSOC was measured with a total organic carbon (TOC) Analyzer (Sievers M9; GE, Milwaukee,
120 WI, USA). All samples were measured in triplicate and the average of the three values was used. HULIS
121 fractions were separated from 38 WSF samples using 6 mL Oasis HLB column (Waters, Milford, MA,
122 USA), and details were presented in the SI. Endotoxins were analyzed using kinetic chromogenic Limulus
123 amoebocyte lysate assay³ (Genscript, USA). Results of WSOC and HULIS were expressed as μg/m³, and
124 endotoxins was expressed as EU/ml, and the blank filter was used as the blank, whose chemicals
125 concentrations were subtracted.

126

127 *2.4 NMR analysis*

128 The proton NMR (¹H NMR) spectra were recorded on an AVANCE III 400 spectrometer (Bruker,
129 Billerica, MA, USA) with an operating frequency of 400.13 MHz. Spectra acquisition was performed with

130 a contact time of 2.27 s and the zg30 pulse program. The recycle delay was 2 s and the proton 90° pulse
131 length was 8.87 μ s. About 200 scans per spectrum were collected. A 1.0 Hz line broadening weighting
132 function and baseline correction were applied. For the NMR analysis, the solid extracts of the samples
133 were dissolved in D₂O. Functional groups in the NMR spectra were identified based on the chemical shift
134 (δ H) relative to that of the water (4.7 ppm). Each spectrum was then manually phase- and
135 baseline-corrected with the chemical shift for the 38 water-soluble samples. The spectral regions of δ
136 0.7–1.9 ppm for aliphatic compounds, δ 1.9–3.2 ppm for unsaturated compounds, δ 3.3–4.5 ppm for
137 carbohydrate compounds, and δ 6.7–8.3 ppm for aromatic hydrogens were based on a previous PM_{2.5}
138 study¹¹. The area of the blank sample was subtracted from each sample, and the NMR value of each
139 functional group was expressed as the proportion of each functional region area to the total area of the four
140 function groups.

141 *2.5 Cell treatment, inflammatory activity analysis, DNA methylation and gene expression analysis*

142 The treatment of A549 and Beas-2B cells were shown in the SI. For comparing the ability of
143 pro-inflammatory release of different PM_{2.5} samples, cells were exposed to the 16.8–90.9 μ g/cm² of PM_{2.5}
144 all collected from 10 m³ of air for 3 days. Cells were harvested after the exposure, and the genomic DNA
145 of the cells was extracted for the DNA methylation test. RNA was also extracted for the gene expression
146 assay²¹, and the cell supernatant was used for interleukin (IL)-6 and IL-8 assays using human IL-6/IL-8
147 Quantikine ELISA kits (R&D Systems, Minneapolis, MN, USA). A blank filter with same area as the
148 sample filter from 10 m³ air was used as the control.

149 *DNA methylation PCR array:* The Xinxiang spring (XXSP) sample, which induced the third highest
150 IL-6 response among the samples, was selected for the PCR array (Lung Cancer DNA Methylation PCR
151 Array; Qiagen, German) for screening candidate genes.

152 *DNA methylation: RASSF2 and CYP1B1* gene methylation was performed using Sequenom
153 MassARRAY method, and *LINE-1* and *iNOS* gene methylation were analyzed using the pyrosequencing
154 method²¹. Details were shown in the SI.

155 The gene expression assay was performed as described in our previous work²¹. And primers are
156 showed in Table S1.

157 *2.6 Statistical analysis*

158 We used the Kruskal–Wallis test to analyze for differences in water-soluble ion/element, WSOC,
159 NMR, HULIS, PM_{2.5}, IL-6, IL-8, DNA methylation, and gene expression levels among the samples from
160 all four seasons and 10 cities. Principal component analysis (PCA) was performed on the PM components.
161 The associations between each chemical (or contributions) and cytokine production were evaluated using
162 Pearson correlation analysis for normally distributed data and Spearman correlation analysis for
163 non-normally distributed data. Relationships were considered to be significant when $p < 0.05$. The data
164 were analyzed with SPSS software (ver. 20.0; IBM Corp, Armonk, NY, USA) (provided by the Chinese
165 Center for Disease Control and Prevention). All biology experiments were carried out four times and three
166 time in chemicals experiments, and the average and median data was used.

167

168 **3. Results and Discussion**

169 *3.1 Characteristics of PM_{2.5} samples*

170 *PM_{2.5} characteristics:* PM_{2.5} concentrations were higher in W and SP than in S and A, but the
171 difference was not significant ($p = 0.184$). Significant differences in PM_{2.5} concentrations were observed
172 among the cities ($p = 0.003$, Table S2). Coastal cities had the lowest concentrations, which may results
173 from more rainwater in coastal cities leading to more atmospheric sedimentation, and also more air flow to

174 the sea comparing to insider cities may also contribute to this result.

175 *Characteristics of inorganic compounds:* Br⁻, PO₄³⁻, and NO₂⁻ were found in very low concentrations
176 and were subsequently disregarded. Northern cities had higher water-soluble ion contents than southern
177 cities ($p = 0.016$) and the average concentration followed the order: NJ > TY > XX > LZ > BJ > SH >
178 GZ > WH > CD > GY. Similarly, water-soluble metal (loid) elements, which accounted for about $0.75 \pm$
179 0.67% of PM_{2.5}, showed significant differences among the cities ($p = 0.004$).

180 Most ions/elements showed higher concentrations in W and A and lower concentrations in SP and S (p
181 < 0.05), except for Pb, which had higher concentrations in SP and S than A and W. A similar trend in Pb
182 was reported in Mexico City³. Based on the current use of electric vehicles, more Pb may leak from Pb
183 batteries in China under higher temperatures in SP and S, which might have contributed to the higher Pb
184 ion concentrations in these seasons. However, more data were needed to explore if battery was the main
185 reason, and other factors might be also contributed to this trend since the concentration of Pb was higher in
186 SP than S. The higher rainfall and temperature in SP and S may have lowered the Cl⁻, NO₃⁻, Na⁺, K⁺, Ca²⁺,
187 and Mg²⁺ concentrations in PM_{2.5}.

188 *Organic compound characteristics:* WSOC accounted for $2.93 \pm 2.83\%$ of PM_{2.5} (m/m), and the
189 concentration of blank filter was $0.0102 \mu\text{g}/\text{m}^3$. The molecular structural characteristics of WSOC were
190 studied using NMR. Based on the recommended method, $\delta^1\text{H}$ 0.7–1.9 ppm (NMR1; *H-C*, representing
191 compounds including protons from methyl, methylene, and methyne groups), $\delta^1\text{H}$ 1.9–3.2 ppm (NMR2;
192 *H-C-C=*, including protons bound to the carbon in the α -position adjacent to a double-bond in allylic,
193 carbonyl, or imino (H-C α -C=O or H-C α -C=N) groups and protons in secondary and tertiary amines), $\delta^1\text{H}$
194 3.3–4.5 ppm (NMR3; *H-C-O*, compounds with protons bound to oxygenated saturated aliphatic carbon
195 atoms in alcohols, polyols, esters, and organic nitrate), and $\delta^1\text{H}$ 6.7–8.3 ppm (NMR4; *Ar-H*, including

196 protons bound to aromatic carbon) were taken to represent different types of non-exchangeable organic
197 hydrogens when analyzed with liquid particulate matter samples¹¹. All groups showed significant
198 differences between the cities and seasons (Kruskal–Wallis test; Table S3), except NMR4 among the cities.

199 The HULIS fractions had high aliphatic (NMR1) and carbohydrate (NMR3) structural characteristics
200 ¹¹. HULIS components were therefore further extracted from the WSFs of PM_{2.5} samples and quantified.
201 The average HULIS concentration was $1.54 \pm 1.64 \mu\text{g}/\text{m}^3$, and concentration of blank filter is $0.0191 \mu\text{g}/\text{m}^3$.
202 Moreover, the proportion of HULIS to WSOC was between $80 \pm 1.66\%$, suggesting HULIS as the main
203 component of WSOC.

204 *3.2 Response of IL-6 and IL-8 to the WSF of PM_{2.5}*

205 First, we compared the ability to induce IL-6 release in A549 cells between the WSF and
206 dichloromethane (DCM)-soluble fraction of five PM_{2.5} samples, and the results indicated that cells exposed
207 to the WSF released more IL-6 than those exposed to the DCM-soluble fraction (Figure S1). During Figure
208 S1, three different PM_{2.5} samples represented three typical sources of pollution: biomass (corn stalk),
209 residential coal combustion (coal), and vehicle exhaust particles (vehicle). PM_{2.5} normally had the highest
210 concentrations in winter, so these five samples were chosen to explore the ability of pro-inflammatory
211 release of WSF fraction in PM_{2.5} than that of DCM fraction. The results may possibly be because the WSF
212 constituted more than 39% of the PM_{2.5} mass. Specifically, the water-soluble inorganic ions, WSOC, and
213 water-soluble metal (loid) elements accounted for about 35%, 3%, and 1% of the PM_{2.5} mass, respectively,
214 while the DCM-soluble fraction accounted for only about 0.1% of the PM_{2.5} mass⁴. Similarly, the WSF
215 were also more likely to induce DNA damage or cytotoxicity than organic compounds in PM_{2.5} and PM₁₀
216 from Mexico City⁵ and Iran⁶. Therefore, we assessed the pro-inflammatory activity of the WSF of PM_{2.5}
217 from 10 large cities in China. The average response was $191.39 \pm 70.13\%$ and $112.70 \pm 19.31\%$ for IL-6

218 and IL-8 compared to the control samples, respectively, and the concentrations of blank filter were
219 43.26±0.56 pg/ml of A549 cells, and 3.67 ±0.89 ng/ml for Beas-2B cells. Using the XXSP sample, we
220 observed a dose-dependent relationship in both A549 cells (Figure S2) and Beas-2B cells (Figure S2),
221 which confirmed that the increase in IL-6 levels in human lung cells was caused by exposure to the WSF
222 of PM_{2.5}. Interestingly, the samples from different cities showed similar trends in terms of their ability to
223 induce IL-6 and IL-8 with a greater response for IL-6 than IL-8 under the same exposure time ($p = 0.045$
224 for IL-6, $p = 0.049$ for IL-8, Table 1, Figure 1). This followed the order GY > XX > CD > BJ > TY > LZ >
225 NJ > GZ > WH > SH for IL-6. The GY, XX and CD samples elicited the greatest response, whereas the GZ,
226 WH, and SH samples elicited the lowest responses (Table 1). Generally, the WSF of PM_{2.5} in northern
227 cities in China induced more IL-6 than that in southern cities, neglecting the GY city due to missing spring
228 and summer samples (Figure 1). This could be because southern China has higher temperature and more
229 rainwater than northern China, leading to less biomass burning for heating, more gas usage for cooking
230 and less incomplete combustion, which can all result in more secondary organic aerosol²². In addition,
231 more rainwater results in more atmospheric washout, which with more air flow to the sea, attribute to
232 better air quality in southern China.

233 Significant variations among the seasons were observed for the IL-6 response, but not the IL-8
234 response ($p = 0.03$ for IL-6, $p = 0.57$ for IL-8, Table 1). In addition, different locations showed different
235 trend for the IL-6 response. For instance, colder seasons samples in BJ, SH, GZ, LZ, and CD were more
236 potent in inducing IL-6 than those from warmer seasons, while in four cities, TY, XX, NJ and WH, SP and
237 S samples were more potent in inducing IL-6 than samples from A and W ($p < 0.05$, Figure 1). These
238 differences in toxicity among cities can be used for better understanding the overall state of PM_{2.5} pollution
239 in China.

240 *3.3 Components of PM_{2.5} associated with pro-inflammatory cytokine release*

241 IL-6 and PCA: No significant correlation was found between mass of PM_{2.5} and IL-6 or IL-8. PCA of
242 water-soluble inorganic ions, and metal (loid) elements, HULIS, non-HULIS, endotoxin, and NMR1-4
243 were performed; 5 factors accounting for 76% of the total variance, were identified (Table S4).

244 PCA1 mainly included Na⁺, Cl⁻, NMR1, NMR2, K⁺, NMR3, Zn, NO₃⁻, NH₄⁺, Mg²⁺, Mn, NMR4,
245 SO₄²⁻, Endotoxin, Co, TI, Cu, Cr, Ca, and As ions; it explained 43% of the total variance, which may be
246 from secondary inorganic aerosol and sea salt. PCA2 mainly included Al, Cr, Fe, Co (negative), Cu, and Pb;
247 it accounted for 12% of the total variance, which may be from industrial sources. PCA3 included NH₄⁺
248 (negative), Ca²⁺, Mg²⁺, and Pb; it represented 9% of the total variance, which may be from road dust
249 sources and formation of NH₄⁺ may be from NO_x catalytic unit of motor vehicle. PCA4 included V
250 (negative), Ni (negative), As, and Cd; it accounted for 8% of the total variance, which may represent ship
251 emissions. PCA5 included HULIS (negative) and non-HULIS; it explained 5% and may represent primary
252 biomass burning, residual coal combustion and secondary organic aerosols.

253 A correlation analysis between pro-inflammatory and the PCA factors showed that there is only a
254 significant correlation between PCA3 (included NH₄⁺, Pb, Ca²⁺, and Mg²⁺) and IL-6 ($r = 0.370$, $p = 0.022$,
255 Table 2) confirmed by linear regression ($B = 0.370$, $p = 0.022$) and multiple linear regression analyses ($B =$
256 0.370 , $p = 0.026$; Table 2). These results suggest that Pb, Mg, and Ca²⁺ were the main components of the
257 WSF of PM_{2.5} that induced IL-6 release, whereas NH₄⁺ may have exerted a negative influence on this
258 process. A linear regression analysis between IL-6 and each ion/element was performed, in which only Pb
259 and IL-6 were significantly correlated ($B = 0.337$, $p = 0.039$; Table 2). Similarly, the Pb standard induced
260 IL-6 in a dose-dependent manner (Figure S3) in A549 cells. These results suggest that Pb may be a
261 non-negligible component of PM_{2.5} for IL-6 induction.

262 In cells exposed to PM_{2.5} from Mexico City, Ca²⁺ showed similar correlation with pro-inflammatory
263 responses with our results³. Moreover, an epidemiological study reported that acute exposure to Pb of
264 PM_{2.5} was associated with negative health effects²³. To date, several water-soluble ions and metal (loid)
265 elements from PM_{2.5} collected in different areas have exhibited a relationship with the pro-inflammatory
266 response. For example, K⁺ showed contrasting effects on the inflammatory response to PM_{2.5} from Milan⁸
267 and North Carolina²⁴, while Si and Al in PM_{2.5} from these two areas exhibited similar effects. In addition,
268 Fe ions in PM₁₀ collected in Milan²⁶ induced a pro-inflammatory response in cells, while the inverse result
269 was reported for PM_{2.5} and PM₁₀ in Mexico City³. Overall, PM from different areas contains similar
270 components but in different proportions, leading to regional variations in toxicity due to complex reactions
271 between components. Therefore, understanding the interactions among individual components of PM is
272 important for identifying the primary toxic components of PM_{2.5}.

273 *IL-6 and endotoxins:* As expected, a significant correlation was noticed between IL-6 and endotoxins
274 ($r = 0.363$, $p = 0.025$), and the linear regression relationship confirmed this correlation ($B = 1.859$, $p =$
275 0.025). Our results also confirmed the idea that endotoxins in PM_{2.5} are important for toxicity³.

276 *IL-6 and organic compounds:* We observed a slight but not significant correlation between IL-6 and
277 WSOC ($r = 0.295$, $p = 0.072$, Pearson correlation analysis), and not IL-8 and WSOC ($r = 0.030$, $p = 0.875$,
278 Spearman correlation analysis). IL-6 and HULIS were significantly correlated ($r = 0.322$, $p = 0.049$; Table
279 2), and the linear regression analysis yielded similar results ($B = 0.322$, $p = 0.049$; Table 2) in A549 cells.
280 Moreover, samples with higher proportions of HULIS induced greater IL-6 release in Beas-2B cells
281 (Figure S4). Finally, the HULIS and non-HULIS fractions were extracted from six PM_{2.5} water-soluble
282 samples. Under the same exposure concentrations, the ability of these fractions to induce IL-6 release
283 followed the order HULIS > WSF > non-HULIS (Figure S4). These results suggest that HULIS might be

284 the main fraction in PM_{2.5} that induced cytokine release. This is the first report of a relationship between
285 HULIS in PM_{2.5} and the cytokine response in a human cell line.

286 HULIS represents a complex class of organic macromolecular compounds, including aromatic and
287 polyacidic molecules. It is reported that HULIS from atmospheric aerosol samples induced ROS in a
288 cell-free DTT assay¹⁰, which is the only direct evidence of HULIS toxicity against reversible redox sites.
289 However, it has been proposed that HULIS is associated with inflammatory and fibrotic lung disease based
290 on the complex host Fe, which initiates inflammation pathways and subsequent fibrosis²⁶. In this study,
291 using human cell line models, the correlation analysis results indicated that HULIS contributed to
292 pro-inflammatory release, and the extracted HULIS fraction results (Figure S4) provided direct evidence
293 confirming this hypothesis. Based on Fourier-transform ion cyclotron resonance mass spectrometry and
294 dual carbon isotope analysis, we previously revealed that primary emissions (i.e., biomass burning and
295 residual coal combustion) and secondary organic formation were important sources of HULIS^{27,28}.
296 Therefore, these two sources should be targeted by air pollution control countermeasures.

297 Here the relationship between the molecular groups and IL-6, NMR1 and NMR3 were significantly
298 correlated with IL-6 release (NMR1 and IL-6: $r = 0.358$, $p = 0.028$; NMR3 and IL-6: $r = 0.333$, $p = 0.041$;
299 Table 2). This suggested that organic species in PM_{2.5} with aliphatic (NMR1, $\delta^1\text{H}$ 0.7–1.9 ppm) and
300 carbohydrate (NMR3, $\delta^1\text{H}$ 3.3–4.5 ppm) structural characteristics might contribute to the IL-6 response.
301 Meanwhile, compounds with characteristics of NMR2 ($\delta^1\text{H}$ 1.9–3.2 ppm) and NMR4 ($\delta^1\text{H}$ 6.7–8.3 ppm)
302 might represent nontoxic components¹¹. Figure 2 presents the spectra of the WSFs of NJ and TY from S
303 and W. IL-6 concentrations were higher in cells exposed to the NJW and TYW samples, and higher NMR1
304 and NMR3 peaks were observed in these two samples compared with the NJS and TYS samples,
305 respectively.

306 Shima reported that hydroxyl and carbonyl functional groups in the n-hexane-insoluble fraction of
307 diesel exhaust particles may have been responsible for the inflammatory response in a rat alveolar
308 epithelial cell line (SV40T2)²⁹. In our previous paper, we reported that hydroxyl groups had an important
309 role in the liver tumor-promoting effect of triclosan²⁰. Therefore, hydroxyl functional groups in the WSF of
310 PM_{2.5} may have played an important role in IL-6 release in this study. This is the first report of the
311 structural characteristics of the toxic fractions of the WSF of PM_{2.5} from 10 large cities in China.

312 Five cities samples (BJ, SH, GZ, LZ, and CD) elicited higher IL-6 response in colder seasons than
313 those of warmer seasons. On the other hand, lower IL-6 release in colder seasons was observed in four
314 cities (TY, XX, WH, and NJ) samples. Generally, in all samples, our data showed that HULIS, Pb, and
315 endotoxins components may be reasons for the IL-6 release for the significant correlation, and NMR1 and
316 NMR3 structural groups also play important roles to pro-inflammatory response. For different cities,
317 different factors may contribute to pro-inflammatory release. For example, for BJ, SH, GZ, and LZ cities,
318 higher HULIS, PCA3, NMR1, and NMR3 may contribute to higher IL-6 release in colder seasons, and for
319 CD city, HULIS, PCA3, NMR1 may lead to this trend. For WH, TY, and XX cities, higher IL-6 release
320 potent in warmer seasons may results from higher NMR3/NMR1 and Pb, however, for NJ city, higher Pb
321 ions may lead to higher IL-6 release in warmer seasons. Similar results of these two different trends were
322 reported through epidemiology and *in vitro* experiments data. For example, PM_{2.5} from BJ city samples
323 showed lower inflammatory release in *in vivo* experimental data³⁰. For the second trend, epidemiology data
324 reported that PM from warmer season showed stronger association with respiratory mortality in different
325 parts of the world³¹, and with daily mortality in Canada³² and U.S.³³. *In vitro* experiments reported that PM
326 collected during S had a greater ability to induce pro-inflammatory activity than samples collected during
327 W in Finland⁷, Mexico City³ and Milan⁸. It is clear that different sampler sites have different seasonal

328 differences in inflammatory, and different components are the main reasons for seasonal difference.

329 Our data showed that IL-8 production was dispersed compared to IL-6 production with no significant
330 correlation with PM_{2.5} constituents. This difference between IL-6 and IL-8 could be because of complex
331 interactions between PM_{2.5} components and modulatory interaction between IL-6 and IL-8³³. Similar results
332 showed that IL-8 has no significant changes after exposure to various combinations of immunomodulatory
333 in monocytes, while significant IL-6 release in this cell was seen³³.

334 A549 cells are a type of lung cancer cells, and Beas-2b cells are normal lung epithelial cells, which
335 are commonly used as the cell model of lung exposure at present. In this experiment, A549 cells were
336 mainly used, and Beas-2B cells were used to verify some conclusions, such as verifying the ability of
337 PM_{2.5} to induce inflammatory cytokines, HULIS was more easily to induce inflammation comparing the
338 ability of non-HULIS, and the ability of PM_{2.5} in northern China induced higher IL-6 than that in southern
339 China. Two cells showed similar trends, while in addition, it was also found that the PM_{2.5} induced change
340 trend was more obvious in A49 cells (Figure S2) than that in Beas-2B cell, which needed further
341 experiments to confirm.

342 *3.4 Mechanisms of IL-6 induction via exposure to the WSF of PM_{2.5}*

343 The DNA methylation inhibitor 5-aza-2'-deoxycytidine (AZA) heightened the ability of the WSF to
344 induce IL-6 release (Figure S5, SI). Therefore, DNA methylation may be a pathway by which WSF
345 exposure upregulated pro-inflammatory cytokines in A549 cells, although the extent of the increase or
346 decrease of major disease-related genes was unknown. Using lung DNA methylation chip, we found only
347 methylation of *CYP1B1* and *RASSF2* differed significantly ($p = 0.021$ for *CYP1B1*, and $p=0.036$ for
348 *RASSF2*, ANOVA) from the control (Figure S6). Therefore, we selected *CYP1B1* and *RASSF2* for further
349 experiment.

350 The MassARRAY assay showed that DNA methylation of *CYP1B1* was significantly decreased
351 compared with blank samples (Table 3) in cells exposed to PM_{2.5} samples, meanwhile, *RASSF2* showed
352 hypermethylation in the CpG islands in its promoter area (Table 3), and DNA methylation of blank filter
353 exposed cells was 30.4% and 10.5% for *CYP1B1* and *RASSF2* genes. Reverse transcription PCR revealed
354 increased *CYP1B1* expression and decreased *RASSF2* expression (Table 3). Both *CYP1B1* and *RASSF2*
355 mRNA expression showed negative correlations with DNA methylation (*CYP1B1*: $r = -0.402$, $p = 0.014$,
356 Pearson correlation analysis; *RASSF2*: $r = -0.325$, $p = 0.032$, Pearson correlation analysis). In addition,
357 significant correlations were found between *CYP1B1* mRNA and IL-6, respectively (*CYP1B1*: $r = 0.286$, p
358 $= 0.049$, Pearson correlation analysis), but not *RASSF2* and IL-6 ($r = -0.305$, $p = 0.062$, Pearson correlation
359 analysis), or between the DNA methylation levels of either gene and IL-6. Overall, the results suggested
360 that DNA methylation changes in the promoter areas of the *RASSF2* and *CYP1B1* genes might have
361 induced abnormal expression of these two genes, in turn contributing to the increase in IL-6 release in cells
362 exposed to the WSF of PM_{2.5}.

363 Hypomethylation of the *iNOS* gene promoter has been reported to have a significant down-regulating
364 effect on PM_{2.5}³⁵. We assessed this relationship *in vitro* using pyrosequencing to analyze *iNOS* promoter
365 gene methylation²⁰. The results showed that *iNOS* exhibited DNA hypomethylation (80.26 ± 38.08 %;
366 Table 3) and but no significantly correlated with IL-6 release ($r = 0.311$, $p = 0.057$, Pearson correlation
367 analysis). Also, there was no significant relationship between *iNOS* mRNA and other chemical components.
368 We also assessed DNA methylation of *LINE-1* to clarify global DNA methylation changes in cells exposed
369 to the WSF of PM_{2.5}²⁰, however, no significant difference was observed between WSF samples exposed
370 cells and the control (100.34 ± 2.63 %).

371 The mechanism of pro-inflammatory cytokine induction are important of PM toxicity, however, there

372 are few reports on it. *CYP1B1* encodes a cytochrome P450 enzyme that is abundant in airway epithelium,
373 and an upregulation of gene expression of this gene was reported in both cells and mice exposed to PAHs
374 and PM³⁶. Meanwhile, *RASSF2* is a potential tumor suppressor gene that might promote apoptosis and cell
375 cycle arrest³⁷, and has shown hypermethylation and downregulated expression in various cancer tissues³⁷.
376 Thus, further work is needed to clarify the pathway of the pro-inflammatory response involving these two
377 genes.

378 Furthermore, IL-6 had a more significant relationship than gene expression/DNA methylation with
379 the components of PM_{2.5}. For example, *CYP1B1* mRNA levels were not correlated with the PCA factors,
380 HULIS, or NMR groups, while IL-6 showed a significant correlation with PCA3, HULIS, NMR1, and
381 NMR3. This might be because gene expression or DNA methylation of *CYP1B1*, *RASSF2*, and *iNOS* may
382 only partially contribute to pro-inflammatory cytokine release. For example, DNA methylation may
383 regulate gene expression, thereby mediating pro-inflammatory release after PM_{2.5} stimulation.
384 Nevertheless, other factors might be involved in this pathway, and data on pro-inflammatory cytokine
385 release can be used to evaluate the PM_{2.5} toxicity, while gene expression and gene modification data can be
386 advised to elucidate the mechanisms of toxicity in *in vitro* studies.

387 Additional studies are needed to further clarify the toxicity of organic-extracted fractions of PM_{2.5}
388 from different cities and seasons in China, to confirm whether the trends in toxicity are similar to those of
389 the WSF of PM_{2.5}. Our results showed that organic compounds might contribute more than other
390 compounds in the WSF of PM_{2.5} to toxicity. HULIS was confirmed as the major toxic component of
391 pro-inflammatory cytokine release; however, the individual compounds of HULIS were not evaluated in
392 terms of their toxicities. Therefore, future work should identify such compounds (e.g., using
393 high-performance liquid chromatography tandem mass spectrometry or Fourier-transform mass

394 spectrometry) to further clarify the chemical characteristics of the NMR3 fractions. Free radicals occur on
395 the surface and inside of PM_{2.5}, which will seize the free radicals on biomacromolecules, may lead to
396 inflammation, cell damage and a series of biological toxicity^{38,39}. Further work is needed to explore the
397 relationship between free radicals and pro-inflammatory release. As another limitation of this study, we
398 pooled every 30 samples to yield the amount of PM_{2.5} required for the toxicity experiments, which reduced
399 the total number of samples. Therefore, future studies should include more samples to perform positive
400 matrix factor analysis and clarify the relationship between PM_{2.5} sources and toxicity, which is important
401 for the development of air pollution control countermeasures.

402

403 **Acknowledgments**

404 The study was supported by Guangzhou Science and Technology Program (201707020033), and
405 Science and Technology Project of Guangdong Province (2014B030301060). We thank Professor Kevin C.
406 Jones in Lancaster Environmental Centre of Lancaster University in the UK for his help in the revision of
407 this manuscript.

408

409 **Conflict of interest**

410 The authors declare no conflict of interest.

411

412 **Supporting Information**

413 Table S1: The primers used in this study; Table S2, S3: Chemical characteristics of WSFs;
414 Table S4: PCA results of the water-soluble inorganic ions, water-soluble elements, HULIS,
415 non-HULIS, endotoxin, and NMR1-4; Figure S1-5: IL-6 response of dichloromethane (DCM)

416 and WSF of PM_{2.5} samples, different concentration of PM_{2.5}, different HULIS fractions,
417 different concentrations of Pb, and DNA Methylation inhibitor; Figure S6: Relative DNA
418 methylation of 22 tumor-related genes in A549 cells exposed to the WSF of PM_{2.5}.

419 **Supporting Methods:** WSF extraction, DCM fraction extraction; Inorganic chemical
420 analyses; HULIS fractions analysis; Cell treatment; DNA methylation and gene expression;
421 PCA analysis.

422

423 **References**

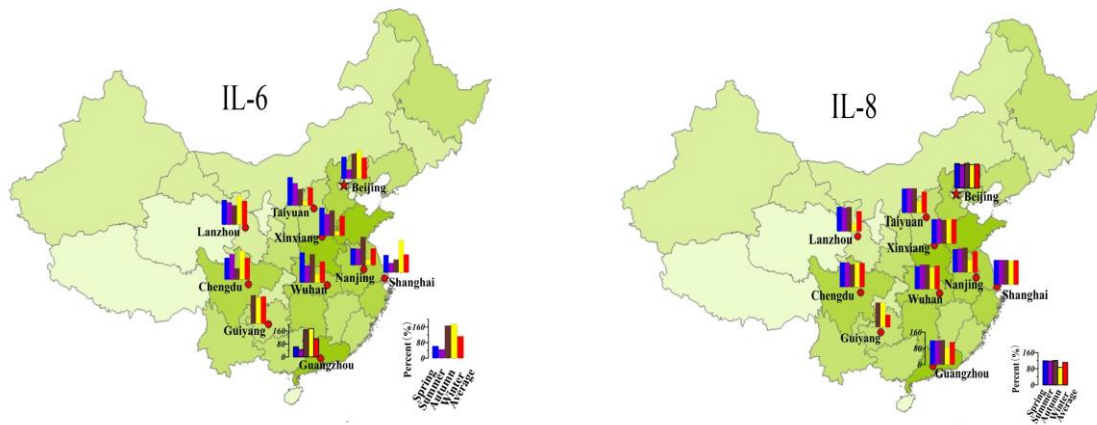
- 424 1. Pope, C. A.; Bhatnagar, A.; McCracken, J.; Abplanalp, W.; Conklin, D. J.; O'Tool, T. Exposure to fine
425 particulate air pollution is associated with endothelial injury and systemic inflammation. *Circ. Res.*
426 **2016**, *119* (11), 1204–1214.
- 427 2. Guastadisegni, C.; Kelly, F. J.; Cassee, F. R.; Gerlofs-Nijland, M. E.; Janssen, N. A.; Pozzi, R.;
428 Brunekreef, B.; Sandström, T.; Mudway, I. Determinants of the proinflammatory action of ambient
429 particulate matter in immortalized murine macrophages. *Environ. Health Perspect.* **2010**, *118* (12),
430 1728-1734.
- 431 3. Manzano-León, N.; Serrano-Lomelin, J.; Sánchez, B.N.; Quintana-Belmares, R.; Vega, E.;
432 Vázquez-López, I.; Rojas-Bracho, L.; López-Villegas, M. T.; Vadillo-Ortega, F.; De, Vizcaya-Ruiz, A.;
433 Perez, I. R.; O'Neill, M. S.; Osornio-Vargas, A. R. TNF α and IL-6 responses to particulate matter in
434 vitro: Variation according to PM size, season, and polycyclic aromatic hydrocarbon and soil content.
435 *Environ. Health Perspect.* **2016**, *124* (4), 406-412.
- 436 4. Tan, J.; Zhang, L.; Zhou, X.; Duan, J.; Li, Y.; Hu, J.; He, K. Chemical characteristics and source
437 apportionment of PM_{2.5} in Lanzhou, China. *Sci. Total Environ.* **2017**, *601-602*, 1743-1752.
- 438 5. Gutiérrez-Castillo, M. E.; Roubicek, D. A.; Cebrián-García, M. E.; De, Vizcaya-Ruiz, A.;
439 Sordo-Cede-o, M.; Ostrosky-Wegman, P. Effect of chemical composition on the induction of DNA
440 damage by urban airborne particulate matter. *Environ. Mol. Mutagen.* **2006**, *47* (3), 199-211.
- 441 6. Naimabadi, A.; Ghadiri, A.; Idani, E.; Babaei, A. A.; Alavi, N.; Shirmardi, M.; Khodadadi, A.;
442 Marzouni, M. B.; Ankali, K. A.; Rouhizadeh, A.; Goudarzi, G. Chemical composition of PM₁₀ and its
443 in vitro toxicological impacts on lung cells during the Middle Eastern Dust (MED) storms in Ahvaz,
444 Iran. *Environ. Pollut.* **2016**, *211*, 316-324.
- 445 7. Jalava, P. I.; Happonen, M. S.; Huttunen, K.; Sillanpää, M.; Hillamo, R.; Salonen, R. O.; Hirvonen, M. R.
446 Chemical and microbial components of urban air PM cause seasonal variation of toxicological activity.
447 *Environ. Toxicol. Pharmacol.* **2015**, *40* (2), 375-387.
- 448 8. Gualtieri, M.; Øvreik, J.; Holme, J. A.; Perrone, M. G.; Bolzacchini, E.; Schwarze, P. E.; Camatini,
449 M. Differences in cytotoxicity versus pro-inflammatory potency of different PM fractions in human
450 epithelial lung cells. *Toxicol. In Vitro* **2010**, *24* (1), 29-39.
- 451 9. Verma, V.; Fang, T.; Xu, L.; Peltier, R. E.; Russell, A. G.; Ng, N. L.; Weber, R. J. Organic aerosols

- 452 associated with the generation of reactive oxygen species (ROS) by water-soluble PM2.5. *Environ.*
453 *Sci. Technol.* **2015**, *49* (7), 4646-4656.
- 454 10. Lin, P.; Yu, J. Z. Generation of reactive oxygen species mediated by humic-like substances in
455 atmospheric aerosols. *Environ. Sci. Technol.* **2011**, *45* (24), 10362-10368.
- 456 11. Chalbot, M. C.; Kavouras, I. G. Nuclear magnetic resonance spectroscopy for determining the
457 functional content of organic aerosols: a review. *Environ. Pollut.* **2014**, *191*, 232-249.
- 458 12. Liu, J.; Han, Y.; Tang, X.; Zhu, J.; Zhu, T. Estimating adult mortality attributable to PM2.5 exposure
459 in China with assimilated PM2.5 concentrations based on a ground monitoring network. *Sci. Total*
460 *Environ.* **2016**, *568*, 1253-1262.
- 461 13. Chen, R.; Qiao, L.; Li, H.; Zhao, Y.; Zhang, Y.; Xu, W.; Wang, C.; Wang, H.; Zhao, Z.; Xu, X.; Hu, H.;
462 Kan, H. Fine paraculate matter constituents, nitric oxide synthase DNA methylation and exhaled nitric
463 oxide. *Environ. Sci. Technol.* **2015**, *49* (19), 11859-11865.
- 464 14. Tarantini, L., Bonzini, M., Apostoli, P., Pegoraro, V., Bollati, V., Marinelli, B., Cantone, L., Rizzo, G.,
465 Hou, L., Schwartz, J., Bertazzi, P., Baccarelli, A. Effects of particulate matter on genomic DNA
466 methylation content and iNOS promoter methylation. *Environ. Health. Perspect.* **2009**, 117:217-222.
- 467 15. Li, J., Zhu, X., Yu, K., Jiang, H., Zhang, Y., Wang, B., Liu, X., Deng, S., Hu, J., Deng, Q., Sun, H.,
468 Guo, H., Zhang, X., Chen, W., Yuan, J., He, M., Bai, Y., Han, X., Liu, B., Liu, C., Guo, Y., Zhang, B.,
469 Zhang, Z., Hu, F., Gao, W., Li, L., Lathrop, M., Laprise, C., Liang, L., Wu, T. Exposure to Polycyclic
470 Aromatic Hydrocarbons and Accelerated DNA Methylation Aging. *Environ. Health. Perspect.* **2018**,
471 126(6):067005.
- 472 16. Bollati, V., Baccarelli, A. Environmental epigenetics. *Heredity* **2010**, 105:105-112.
- 473 17. Zhong, J., Karlsson, O., Wang, G., Li, J., Guo, Y., Lin, X., Zemplenyi, M., Sanchez-Guerra, M.,
474 Trevisi, L., Urch, B., Speck, M., Liang, L., Coull, B., Koutrakis, P., Silverman, F., Gold, D., Wu, T.,
475 Baccarelli, A. B vitamins attenuate the epigenetic effects of ambient fine particles in a pilot human
476 intervention trial. *Proc. Natl. Acad. Sci. USA.* **2017**, 114:3503-3508.
- 477 18. Liu, D.; Lin, T.; Shen, K.; Li, J.; Yu, Z.; Zhang, G. Occurrence and concentrations of halogenated
478 flame retardants in the atmospheric fine particles in Chinese cities. *Environ. Sci. Technol.* **2016**, *50*
479 (18), 9846-9854.
- 480 19. Zhang, X., Li, J., Mo, Y., Shen, C., Ding, P., Wang, N., Zhu, S., Cheng, Z., He, J., Tian, Y., Gao, S.,
481 Zhou, Y., Tian, C., Chen, Y., Zhang, G. Isolation and radiocarbon analysis of elemental carbon in

- 482 atmospheric aerosols using hydroxyprolysis. *Atmos. Environ.* **2019**, 381-386.
- 483 20. Zeng, L.; Ma, H.; Pan, S.; You, J.; Zhang, G.; Yu, Z.; Sheng, G.; Fu, J. LINE-1 gene hypomethylation
484 and p16 gene hypermethylation in HepG2 cells induced by low-dose and long-term triclosan exposure:
485 The role of hydroxyl group. *Toxicol. In Vitro* **2016**, *34*, 35-44.
- 486 21. Ma, H.; Zheng, L.; Li, Y.; Pan, S.; Hu, J.; Yu, Z.; Zhang, G.; Sheng, G.; Fu, J. Triclosan reduces the
487 levels of global DNA methylation in HepG2 cells. *Chemosphere* **2013**, *90* (3), 1023-1029.
- 488 22. George, I. J.; Hays, M. D.; Herrington, J. S.; Preston, W.; Snow, R.; Faircloth, J.; George, B. J.; Long,
489 T.; Baldauf, R. W. Effects of cold temperature and ethanol content on VOC Emissions from light-duty
490 gasoline vehicles. *Environ. Sci. Technol.* **2015**, *49* (21), 13067-13074.
- 491 23. Heo, J.; Schauer, J. J.; Yi, O.; Paek, D.; Kim, H.; Yi, S. M. Fine particle air pollution and mortality:
492 importance of specific sources and chemical species. *Epidemiology* **2014**, *25* (3), 379-388.
- 493 24. Becker, S.; Dailey, L. A.; Soukup, J. M.; Grambow, S. C.; Devlin, R. B.; Huang, Y. C. Seasonal
494 variations in air pollution particle-induced inflammatory mediator release and oxidative stress.
495 *Environ. Health Perspect.* **2005**, *113* (8), 1032-1038.
- 496 25. Camatini, M.; Corvaja, V.; Pezzolato, E.; Mantecca, P.; Gualtieri, M. PM10-biogenic fraction drives
497 the seasonal variation of proinflammatory response in A549 cells. *Environ. Toxicol.* **2012**, *27* (2),
498 63-73.
- 499 26. Ghio, A. J.; Madden, M. C. Human lung injury following exposure to humic substances and
500 humic-like substances. *Environ. Geochem. Health* **2017**, *40* (2), 571-581.
- 501 27. Mo, Y.; Li, J.; Jiang, B.; Su, T.; Geng, X.; Liu, J.; Jiang, H.; Shen, C.; Ding, P.; Zhong, G.; Cheng, Z.;
502 Liao, Y.; Tian, C.; Chen, Y.; Zhang, G. Sources, compositions, and optical properties of humic-like
503 substances in Beijing during the 2014 APEC summit: Results from dual carbon isotope and
504 Fourier-transform ion cyclotron resonance mass spectrometry analyses. *Environ. Pollut.* **2018**, *239*,
505 322-331.
- 506 28. Song J.; Li M.; Jiang B.; Wei S.; Fan X.; Peng P. Molecular characterization of water-soluble humic
507 like substances in smoke particles emitted from combustion of biomass materials and coal using
508 ultrahigh-resolution electrospray ionization fourier transform ion cyclotron resonance mass
509 spectrometry. *Environ. Sci. Technol.* **2018**, *52*(2), 2575-2585.
- 510 29. Shima, H.; Koike, E.; Shinohara, R.; Kobayashi, T. Oxidative ability and toxicity of n-hexane
511 insoluble fraction of diesel exhaust particles. *Toxicol. Sci.* **2006**, *91* (1), 218-226.

- 512 30. Pardo, M.; Xu, F.; Qiu, X.; Zhu, T.; Rudich, Y. Seasonal variations in fine particle composition from
513 Beijing prompt oxidative stress response in mouse lung and liver. *Sci. Total Environ.* **2018**, *626*,
514 147-155.
- 515 31. Stieb, D. M.; Judek, S.; Burnett, R. T. Meta-analysis of time series studies of air pollution and
516 mortality: effects of gases and particles and the influence of cause of death, age, and season. *J. Air*
517 *Waste Manag. Assoc.* **2002**, *52* (4), 470–484.
- 518 32. Goldberg, M. S.; Burnett, R. T.; Valois, M. F.; Flegel, K.; Rd, B. J.; Brook, J.; Vincent, R.; Radon, K.
519 Associations between ambient air pollution and daily mortality among persons with congestive heart
520 failure. *Environ. Res.* **2003**, *91* (1), 8-20.
- 521 33. Moolgavkar, S. H. Air pollution and daily mortality in two U.S. counties: season-specific analyses and
522 exposure-response relationships. *Inhal. Toxicol.* **2003**, *15* (9), 877–907.
- 523 34. Raspé, C.; Czeslick, E.; Weimann, A.; Schinke, C.; Leimert, A.; Kellner, P.; Simm, A.; Bucher, M.;
524 Sablotzki, A. Glutamine and alanine-induced differential expression of intracellular IL-6, IL-8, and
525 TNF- α in LPS-stimulated monocytes in human whole-blood. *Cytokine* **2013**, *62* (1), 52-57.
- 526 35. Jiménez-Garza, O.; Guo, L.; Byun, H. M.; Carrieri, M.; Bartolucci, G. B.; Zhong, J.; Baccarelli, A. A.
527 Promoter methylation status in genes related with inflammation, nitrosative stress and xenobiotic
528 metabolism in low-level benzene exposure: Searching for biomarkers of oncogenesis. *Food Chem.*
529 *Toxicol.* **2017**, *109* (1), 669-676.
- 530 36. Farina, F.; Sancini, G.; Mantecca, P.; Gallinotti, D.; Camatini, M.; Palestini, P. The acute toxic effects
531 of particulate matter in mouse lung are related to size and season of collection. *Toxicol. Lett.* **2011**,
532 *202* (3), 209-217.
- 533 37. Kanwal, S.; Jamil, F.; Ali, A.; Sehgal, S. A. Comparative modeling, molecular docking, and revealing
534 of potential binding pockets of RASSF2; a candidate cancer gene. *Interdiscip. Sci.* **2017**, *9* (2),
535 214-223.
- 536 38. Valavanidis, A., Fiotakis, K., Vlachogianni, T. Airborne particulate matter and human health:
537 toxicological assessment and importance of size and composition of particles for oxidative damage
538 and carcinogenic mechanisms. *J Environ Sci Health C Environ Carcinog Ecotoxicol Rev.* **2008**
539 26(4):339-62.

- 540 39. Dellinger, B., Pryor, W., Cueto, R., Squadrito, G., Hegde, V., Deutsch, W. Role of free radicals in the
541 toxicity of airborne fine particulate matter. *Chem Res Toxicol.* **2001** 14(10):1371-1377.
542



544

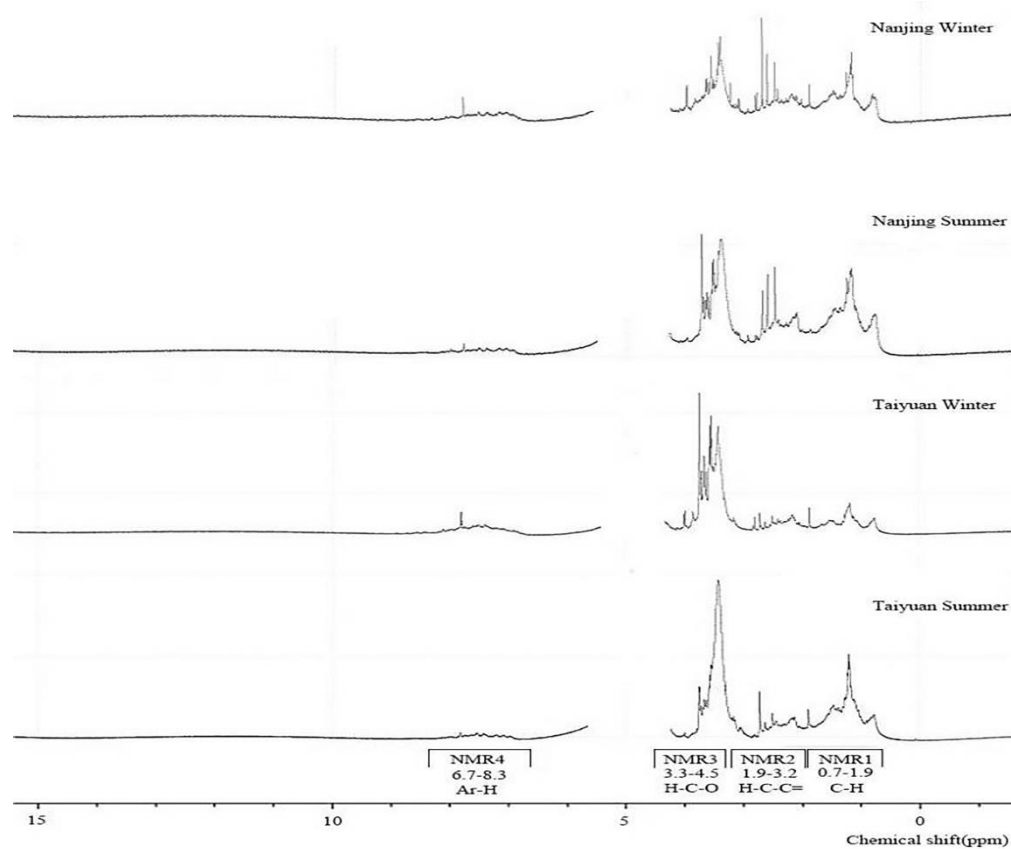
545

546

547 Figure 1. Relative interleukin (IL)-6 and IL-8 response in A549 cells exposed for 3 days to
 548 the water-soluble fraction (WSF) of fine particulate matter (PM_{2.5}) collected in 10 large cities
 549 in China during all four seasons. The WSFs were derived from the same volume of air (10 m³)
 550 and the concentrations were 0.35–10.32 µg/cm². Blank samples that underwent the same
 551 sample treatment were used as the control, which was considered as 100%. Pictures were
 552 drawn using ArcGIS 10.2 software, and the base map of China was from
 553 <http://www.arcgisonline.cn/arcgis/home/item.html?id=a2071f54e2434e0384b8ffab75a19771>.

554

555



557

558 Figure 2. The proton nuclear magnetic resonance (^1H NMR) spectra of the WSFs of the
 559 Guangzhou summer (GZS), Guangzhou winter (GZW), Taiyuan summer (TYS), and Taiyuan
 560 winter (TYW) $\text{PM}_{2.5}$ samples. The region between $\delta^1\text{H}$ 4.0 and $\delta^1\text{H}$ 5.0 was ignored because
 561 of the residual signal of deuterium protium oxide. The four regions (NMR1–4) considered in
 562 this study, and the identified chemical groups, are shown in the figure.

563

564 Table 1. Cytokine production in response to the WSF of PM_{2.5} collected from 10 large
 565 cities in China during 1 year, listed in descending order according to the median values.
 566

	IL-6*			IL-8*	
	Median	Mean±SD		Median	Mean±SD
GY	249.0	249.0±2.791	GY	121.3	121.3±0.1356
XX	247.2	207.7±50.06	XX	121.1	120.1±1.932
CD	233.7	201.8±35.52	CD	120.5	118.5±3.820
LZ	233.2	221.6±30.2	TY	120.4	104.3±31.24
BJ	224.4	195.3±34.56	LZ	118.6	99.40±40.55
NJ	182.6	158.9±57.06	GZ	118.5	111.3±14.60
TY	173.3	147.4±54.65	BJ	118.5	118.2±2.621
GZ	136.4	141.8±70.33	WH	117.0	115.4±6.400
SH	132.9	132.4±56.49	NJ	114.8	102.9±27.58
WH	130.5	139.0±66.49	SH	78.87	84.22±28.40
	IL-6*			IL-8	
	Median	Mean±SD		Median	Mean±SD
Spring	235.8	218.7±28.00	Autumn	121.0	119.7±2.620
Summer	206.3	167.6±57.00	Summer	121.0	119.0±2.310
Winter	189.0	145.8±63.57	Spring	120.8	119.0±2.870
Autumn	170.6	174.7±35.30	Winter	111.0	94.34±33.49

567
 568 **p* < 0.05, Kruskal–Wallis test. Blank samples were used as the control, which was
 569 considered as 100%. GY, Guiyang; XX, Xinxiang; CD, Chengdu; LZ, Lanzhou; BJ, Beijing;
 570 NJ, Nanjing; TY, Taiyuan; GZ, Guangzhou; SH, Shanghai; WH, Wuhan; IL, interleukin
 571
 572

573
574
575

Table 2.

IL-6 ^a		
	<i>r</i>	<i>p</i>
PCA3	0.370	0.022
HULIS	0.322	0.049
Endoxin	0.363	0.025
Pb	0.337	0.039
NMR1	0.358	0.028
NMR3	0.333	0.041
^b linear analysis		
	<i>B</i>	<i>p</i>
PCA3	0.370	0.022
HULIS	0.322	0.049
Endoxin	1.859	0.025
Pb	0.337	0.039
^c multiply linear analysis		
	<i>B</i>	<i>p</i>
PCA3	0.370	0.026

576
577
578
579

HULIS, humic-like substances; NMR, nuclear magnetic resonance.

Note: ^a Correlation analysis. ^b Multiple linear regression model, in which the five principal components (PCA1, PCA2, PCA3, PCA4, and PCA5) were independent variables.

580 Table 3: DNA methylation and expression of several genes in A549 cells exposed to the WSF of PM_{2.5} samples.

	<i>RASSF2</i> DNA	<i>CYP1B1</i> DNA	<i>iNOS</i> DNA	<i>LINE-1</i> DNA	<i>RASSF2</i> mRNA	<i>CYP1B1</i> mRNA	<i>iNOS</i> mRNA
City	methylation	methylation	methylation	methylation			
BJ	126.1±36.86	88.89±22.78	97.56±20.36	99.55±1.680	92.90±34.56	220.4±114.2	124.9±56.32
SH	106.9±2.201	83.79±24.02	63.34±43.05	100.3±3.282	88.01±12.38	185.2±90.15	162.5±172.8
GZ	121.2±78.25	96.15±8.780	53.21±35.73	99.77±2.720	96.06±8.930	184.3±96.29	481.2±504.7
NJ	124.6±43.13	95.16±9.12	96.44±73.58	101.5±3.292	86.47±21.98	271.9±78.54	297.8±216.5
CD	103.8±38.07	93.12±19.46	81.93±18.48	100.6±1.653	89.08±48.52	227.7±128.3	156.6±65.73
WH	130.2±30.68	91.49±7.182	71.58±47.69	99.61±2.223	99.79±5.310	239.9±61.30	126.7±31.58
LZ	131.6±57.45	82.85±26.38	75.69±17.04	101.3±2.070	83.74±35.26	318.3±300.6	162.0±86.58
GY	142.8±21.53	82.11±7.200	54.11±74.76	97.23±3.710	82.25±22.30	253.4±128.6	156.9±80.92
TY	158.4±70.42	98.13±7.560	91.00±18.82	103.6±2.300	69.53±22.83	299.8±141.6	115.4±64.02
XX	107.0±13.41	94.30±12.42	104.6±12.87	98.56±1.441	87.83±28.72	260.4±120.1	155.2±110.1
Season							
spring	114.2±41.01*	95.33±3.73*	76.39±55.78*	99.84±2.350	87.09±19.67*	250.4±80.80*	186.2±120.7
summer	152.7±43.93*	88.81±8.82*	89.55±11.32*	101.6±1.690	83.93±32.76*	202.9±111.1*	149.9±69.09
autumn	104.4±26.11*	98.49±8.200*	100.6±19.28*	101.3±1.630	103.1±13.21*	175.3±68.06*	286.1±355.1
winter	129.6±52.75*	75.30±17.98*	54.98±37.92*	98.76±3.580	88.40±26.00*	350.6±170.9*	155.7±128.1
average	119.1±46.61*	92.02±16.07*	80.25±38.08*	100.3±2.63	89.76±23.62*	245.7±130.7*	195.9±205.0

581 **p* < 0.05, ANOVA. BJ, Beijing; SH, Shanghai; GZ, Guangzhou; NJ, Nanjing; CD, Chengdu; WH, Wuhan; LZ, Lanzhou; GY, Guiyang; TY,
582 Taiyuan; XX, Xinxiang. Cells were exposed in WSF from 10 m³ air. Blank samples that underwent the same sample treatment were used as the
583 control, which was considered as 100%, and DNA methylation and gene expression of each gene was expressed as relative DNA
584 methylation/gene expression comparing to control.